17th Australasian Fluid Mechanics Conference
Auckland, New Zealand
5-9 December 2010

Practical CFD to Compute Resistance, Sink and Trim of Fully Appended Sailing Yachts

I.M. Viola[1] and R.G.J. Flay[1]

[1]Yacht Research Unit, University of Auckland, Auckland 1142, New Zealand

Abstract

The Computational Fluid Dynamics analysis of the hydrodynamic performance of two America's Cup design candidates is presented. Two fully appended hulls were tested in a *free to sink and trim* condition. The experimental data of one of the two hulls was known *a priori* and was used to investigate several computational parameters, which are discussed in the present paper. The validated numerical model was used to predict the performance of the second hull, whose experimental data were unknown *a priori*. The *a posteriori* numerical/experimental comparison showed that the numerical model was able to predict the performance of the two hulls with a level of accuracy of the same order of magnitude of the experimental test.

Introduction

"Practical CFD" in yacht design practice, which is achievable with reasonable computational resources, is a compromise between the computational effort and the accuracy of the result. The accuracy in the computation of hull resistance required by yacht designers is of $O(1\%)$, which is also the order of magnitude of the repeatability of the towing tank [2]. Hence, "practical CFD" should be able to predict the resistance of a yacht with the accuracy of the order of 1%. It was proven [3] that this level of accuracy can be achieved with "practical CFD", which adopt turbulence models, wall functions, low grid resolution, large time steps, low time and space discretization orders. However, the "practical" nature of these simulations leads to different results when different choices are made, in terms of grid resolution, time step, etc. Hence, a validation procedure should be performed very carefully. In particular, the numerical/experimental comparison of the resistance of one hull is not sufficient to prove the accuracy of the model, because a specific set of chosen parameters might lead to the sum of large positive and large negative errors, giving a small overall error. Conversely, a good "practical CFD" should achieve a small overall error, resulting the sum of small errors. A validation procedure should show that the overall error is sufficiently small, in the design range of different conditions and geometries, to allow the resistance, and the sink and trim to be predicted with the required accuracy without knowing the experimental results *a priori*.

Method

An America's Cup (AC) team provided the Yacht Research Unit (YRU) with two geometries, both candidates of the 32nd America's Cup. Figure 1 shows the main dimensions of the two geometries, named TH04 and TH06 respectively. The AC team provided the YRU with the towing tank data for TH04 but, until the end of the project, did not provide the towing tank data for TH06.

Experimental Method

The towing tank tests were performed on 1/4th scale model hulls in *free to sink and trim* conditions and in calm water. Boat speeds *(BS)* from 6 to 12 knots full-scale were tested, meaning from 3 to 6 knots model-scale. In fact, the *BS* was scaled with the aim of keeping the same Froude number *(Fr)* at full-scale and model-scale. The models were fully appended, and zero leeway angle and zero heel angle were used.

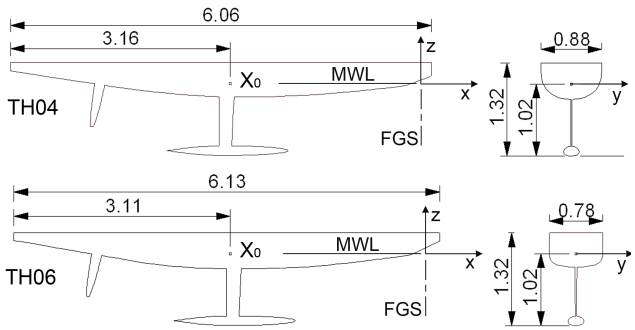

Figure 1: Main dimensions of the two geometries tested.

Numerical Method

The commercial code STAR-CCM+ (CD-adapco) version 4.06.011 was used. The model-scale experiments were modelled.

The incompressible Navier-Stokes equations were solved with an implicit unsteady solver. Both air and water densities were assumed to be constant. The second-order in space and first-order in time was used to solve the discrete system. The κ–ε *realizable* turbulent model was used. Several grids were tested but none of them solved the boundary layer along all the hull and the appendages. Therefore, the boundary layer was modelled with wall functions. The *two-layer all* y^+ *wall treatment* was used (see *User Guide STAR-CCM+ Version 4.06.011* for details). The *all* y^+ formulation switches from the traditional wall-function approach to the traditional low-Reynolds number approach, using a blending function g, which is function of the Reynolds number based on wall distance. The *two-layer* formulation for the κ–ε *realizable* turbulent model, switches to a one-equation model in the near-wall region, which solves κ but prescribes algebraically ε, as a function of the wall distance. A *volume of fluid (VOF)* technique was used to model the two-phases, air and water.

Results and Discussion

Grids

Two grid types were tested. Hexahedral non-structured non-conformal grids were made with STAR-CCM+ (CD-adapco), and block-structured conformal grids were made with ICEM-CFD (Ansys). It should be noted that STAR-CCM+ is a face-based non-structured solver. Hence, the terms non-conformal and structured are referred to the grids and not to the way that the solver manages the grids.

In the non-structured non-conformal grids, performed with STAR-CCM+, the domain is filled with hexahedra, which are trimmed by the hull. Each hexahedron can be halved in any of its

sides. The boundary layer is modelled with prismatic cells. The method is very interesting because it allows automatic grid generation, which is an important feature to use to compare different geometries. This approach allows the grid resolution to be increased on the wave pattern, without increasing excessively the overall number of cells.

In the block-structured conformal grids, performed with ICEM-CFD, the domain is divided into blocks. This approach allows a squared surface grid to be achieved, where the edges are aligned with the main flow direction, which improves the computation of the fluid in the boundary layer.

The two approaches were investigated with several different grids for TH04, with various numbers of cells and various criteria for grid refinement. It was found that roughly 700,000 cells are the minimum number of cells to model half the hull. Increasing the number of cells up to roughly 2,000,000 cells leads to a larger difference between the computed resistance and the measured resistance at each *BS* (named "absolute difference" in the following). Conversely, the difference between the computed and the measured delta resistance between two *BS* decreases (named "relative difference" in the following). The absolute difference increase with low resolution is due to the sum of positive and negative errors cancelling out. In particular, modelling the boundary layer with low grid resolution causes the friction resistance to be over-estimated. Conversely, modelling the wave pattern with low grid resolution leads to a smoother wave pattern and, hence, the pressure resistance is under-estimated. However, this latter effect is generally less significant than the former. Therefore, if all the domain cells were halved, the resistance would be expected to decrease. When high grid resolution was used and a grid independent solution was achieved, the absolute resistance was under-estimated, due to the second-order difference equation, as discussed in the following.

The wall-distance of the first cell centre $y+$ was investigated between $y+=30$ and $y+=300$. It was found that the friction drag decreased asymptotically when y+ decreases. Hence, $y+=30$ or near values are recommended. Lower $y+$ value requires very fine grids or highly stretched hexahedra. Moreover, lower $y+$ causes the *numerical ventilation,* which is discussed below, to increase. For these reasons, the results presented in the following were achieved with $y+=30$.

Discretization Order

First order was used for the transient terms (Euler Implicit). In fact, using second order led to instabilities on the water surface. Conversely, the second order was found to be the most appropriate for the convection terms of the fluid, turbulence and VOF equations. Modelling the convection terms with the first order has 3 undesirable consequences. Firstly, the computed resistance increases due to the increase in numerical diffusion. Secondly, the *numerical ventilation*, which is described in the following, increases. Finally, the thickness of the region where the cells have a mix of the two phases enlarges. In fact, when second order method is used, the transition between the air and the water occurs in a couple of cells, while when first order is used, transition occurs in a larger number of cells, which is due to the numerical diffusion of vof_{water} and vof_{air}.

A test simulation was performed with different discretization orders for the convection term of the VOF, turbulence and fluid equations respectively. The resistance computed using first order for only one of the VOF, turbulence and fluid equations, were 6%, 27% and 30% respectively, larger than when using the second order for all the equations. Finally, the resistance computed using the first order for the convection term of all the equations was 41% larger than when using the second order. However, simulations performed with second order under-estimated the hull resistance. Other authors (e.g. [1]) reported the resistance to be systematically underestimated with a second order scheme. In particular, a blending function between a first-order upwind scheme and second order centred scheme was used. It was found that the resistance decreases linearly from first to second order; first order largely over-estimates the resistance, whereas second order slightly under-estimates the resistance.

6DOF

The sink and trim were modelled with a rigid translation of the whole domain. Hence the boundary conditions were updated at each time step. It was found that the boundary condition variation leads to fluctuations of the water plane height, which are transported through the domain and this can affect the convergence of the simulation. In particular, in the first few seconds, the hull moves from the initial position to the equilibrium position. The inertia forces cause the hull to go past the equilibrium position. The boat reaches the equilibrium position with a damped oscillatory movement. The movements of the hull are modelled by updating the inlet boundary conditions. For instance, the water plane at the inlet is raised up when the hull is sunk. Therefore, the oscillations of the hull lead the inlet boundary condition to oscillate. For instance, figure 2 shows a schematic drawing of the first 2 seconds of one of the simulations performed. At $t=0.0$s the boat is set at a raised position compared to the final state. At $t=0.3$s, the stern is sunk more than the bow, leading to a negative (bow-up) trim. Therefore, the water plane is set to $z=-z_1$ at the boundary inlet. At $t=1.2$s the boat sinks to the final position but the bow sinks more than the stern. Hence, the boat is correctly sunk but has a positive trim. Therefore, the water plane at the boundary inlet is set to $z=z_2$. Finally, at $t=2.0$s the bow is risen up to the final position. Hence, the boat is sunk and has negative trim. During 1.7s=2.0s-0.3s, the height of the water plane at the boundary inlet was oscillating with an amplitude of $\Delta z=z_2-z_1$. As a consequence, a wave with the period of $T\approx1.7$s and a wavelength of $\lambda=BS\cdot T\approx5$m (being $BS=3$m/s), is moving along the computational domain. In this example, after 2.0s the hull had reached the equilibrium position but had to face a wave with a wavelength equal to its water length.

In conclusion, the initial oscillations of the sink and trim of the hull caused the height of the water plane at the boundary inlet to oscillate. This oscillation introduces a wave in the computational domain, which can induce a further oscillation of the sink and trim of the hull. This wave can significantly affect the convergence. To minimise the wave amplitude due to the trim oscillation, the upstream inlet face should be as close as possible to the boat. In the present paper, one boat length was used. If the final sink and trim are known, these values should be used as the initial conditions. When the trim is modelled, the pitching inertia can be used to speed up the convergence.

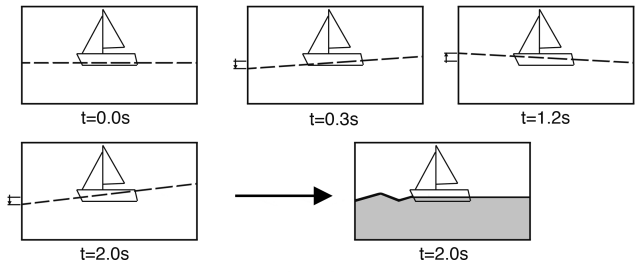

Figure 2: Schematic drawing of wave generation due to sink and trim initial oscillations

Skin Friction

The computation of skin friction is often affected by *numerical ventilation*, which occurs when particles of air are trapped into

the boundary layer and transported below the water plane. This problem is well known in the field by users and CFD vendors. However, it has rarely been mentioned or discussed in scientific publications. The amount of air in the boundary layer depends on the grid resolution, on the hull geometry and on the *BS*. Air is located in only the first few cells near the wall. Therefore, the air is confined in a very small fraction of the boundary layer thickness. However, the shear stress is incorrectly computed using properties of this mixed fluid, instead of for the fluid with water properties.

The wall function computes the friction velocity u^* using the following equation:

$$u^* = \sqrt{g \cdot \frac{\nu u}{y} + (1-g) \cdot C_\mu^{1/2} \cdot k} \qquad (1)$$

Where $g = \exp\left(-\frac{1}{11} \cdot \mathrm{Re}_y\right)$ is the *all-y*$^+$ blending function, $\mathrm{Re}_y = \sqrt{k}\frac{y}{\nu}$ is a wall-distance-based Reynolds number, ν is the kinematic viscosity, u is the tangential velocity, y is the wall distance, C_μ=0.09 is a constant, and k is the turbulent kinematic energy.

Equation (1) shows that u^* is over-estimated when numerical ventilation occurs. In fact ν of the mixed fluid is higher than ν for the water. However, the effect of ν is smoothed by the blending function g and becomes negligible for low-resolution grids (because Re_y is large and $g \approx 0$). The wall function also computes a production term for k and algebraically prescribes the value of the turbulent dissipation rate ε, which are both functions of u^*. When low-resolution grids are adopted, these terms are not affected significantly by the numerical ventilation, because the over-estimation of u^* is negligible. In the present paper, and in most of the engineering applications in this field, the grid resolution in the near-wall region is low (typically $y^+ > 30$), and hence the over-estimation of u^* is negligible.

The shear *stress* τ_w *is* computed from u^* by the following equations:

$$\tau_w = \rho \cdot (u^*)^2 \qquad (2)$$

Equation (2) shows that, if the error in the computation of u^* is negligible, the shear stress is under-estimated due to numerical ventilation. The error in estimating the shear stress is proportional to the vof_{air}. In fact from equations (2):

$$\tau_w = (vof_{air} \cdot \rho_{air} + vof_{water} \cdot \rho_{water}) \cdot (u^*)^2 = \\ = \tau_{w\_water} - vof_{air} \cdot (\rho_{water} - \rho_{air}) \cdot (u^*)^2 \qquad (3)$$

Equation (3) suggests that the shear stress computed by the solver τ_w could be corrected by adding the last term of the equation.

In the present paper, the skin friction resistance σ was computed by integrating u^* on the wetted surface A_w and than multiplying it by the water density as shown in Equation (4).

$$\sigma = \rho_{water} \cdot \int_{A_w} (u^*)^2 \qquad (4)$$

This method does not take into account the over-estimation of u^* due to the wall function. Hence, this method is not suitable if the grid in the boundary layer is highly refined.

Aw should be opportunely defined considering the shape of the bow waves. In fact, the transition between air and water should occur in only one or two cells. Conversely, transition occurs in a large number of cells in the region of the bow wave. Downstream of the bow wave, a high grid resolution allows transition to occur again in only one or two cells. It is common practice to define the free surface with an iso-surface where $vof_{water}=vof_{air}=0.5$. However, due to numerical diffusion, which increases the amount of air in the mixed fluid, a lower value of vof_{water} can be considered. A lower value of vof_{water} significantly affects the region of the bow wave where the transition between $vof_{water}=0$ and $vof_{water}=1$ occurs in several cells, while it is negligible downstream and in the rest of the wave pattern. In the present paper, values between 0.2 and 0.5 were considered for different amount of numerical ventilation.

Time Step

Time steps from *ts*=0.02s to *ts*=0.0001s were tested. The grid size in the stream-wise direction is roughly 0.03m and 0.01m on the hull and on the keel respectively. Hence the Courant numbers, *Co,* based on the *BS* were between *Co=0.1* and *Co*=12. *Co* larger than 12 and smaller than *0.1* lead the simulation to diverge. Decreasing the time step causes the numerical ventilation to decrease. The friction drag increases by about 1% when *ts* is halved, while the pressure drag is constant. In the present paper, for both TH04 and TH06, at *Fr*=0.22 and *Fr*=0.44, the drag was computed with *ts*=0.05 and *ts*=0.0025. The 8 simulations showed that when the friction drag is re-computed to take into account the numerical ventilation as shown above, the friction drag decreases by roughly 1% by halving the *ts*. This latter trend is consistent with the assumption that the friction drag decreases when the numerical diffusion decreases.

Numerical/Experimental Comparison

A grid of 2,250,000 elements was used to model half domain. In fact, as expected, simulations of the whole domain and of only half the domain gave the same results. Hence only the half domain was modelled to save computational time. The simulations performed on TH04 with the grids made with STAR-CCM+ and ICEM-CFD gave very similar results. Thus it was arbitrary decided to perform the comparison with the two grids built with ICEM-CFD. However, similar results were expected if the two grids built with STAR-CCM+ had been used. A *ts*=0.005 with 5 inner iterations was adopted.

The computed drag, sink and trim were in good agreement with the experimental data. Figure 3 shows the numerical and the experimental drag of TH04 at various *BS*. The relative drag differences between various speeds of TH04 showed a numerical/experimental agreement of ±0.8% in the experimental drag. The absolute shift between the numerical and the experimental drag was 0.4% of the experimental drag. The relative trim differences between various speeds of TH04 showed a numerical/experimental agreement of ±0.01 deg. The absolute shift between the numerical and the experimental trim was 0.43 deg. Hence, this shift is probably due to a difference in the zero measurements. In fact, while the angle between two trims can be easily measured, the angle between the trim and the nominal waterplane in measurement condition (MWL) can easily lead to an error of 0.5 degree. Similarly, the relative sink differences between various speeds of TH04 have a numerical/experimental agreement of ±1.2 mm, while the absolute shift between the numerical and the experimental trim was 14.4 mm, which was probably due to a different zero-reference in the experimental measurement.

Comparison of TH04 versus TH06

The comparison between TH04 and TH06 was performed with the same numerical conditions (grid resolution, time step, discretization order, etc.).

The numerical/experimental agreement for TH06 was lower than for TH04, but was still satisfactory. The relative drag differences

between various speeds showed a numerical/experimental agreement of ±0.9% of the experimental drag. The absolute shift between the numerical and the experimental drag was 2.5% of the experimental drag. The relative differences between various speeds for the sink and the trim showed a numerical/experimental agreement of ±0.03 deg and ±1.8 mm, respectively. Plots of numerical/experimental comparisons of the drag, sink and trim, of TH06 are not presented due to space limitations.

Figure 4 shows the drag difference between the two geometries at various full-scale boat speeds. CFD predicted the cross-over just below 10 knots, while the towing tank showed the cross-over just above 10 knots. Hence, the numerical and the experimental results would have led to the same choice between the two geometries at every *BS*, except at 10 knots. The differences between the numerical and the experimental resistance for each hull are of the same order of magnitude of the accuracy of the experimental measurements. Hence the choice of the fastest hull at 10 knots is questionable.

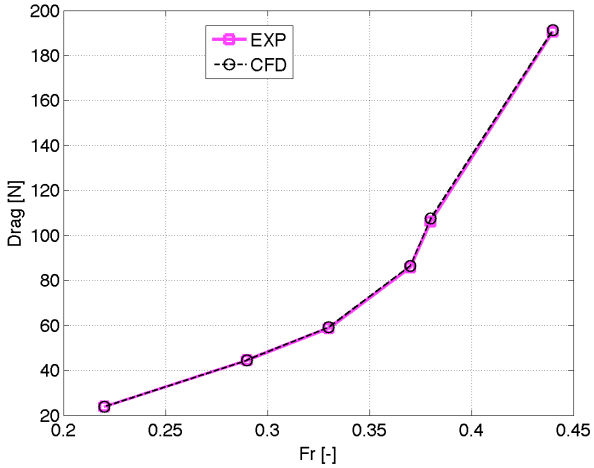

Figure 3: Numerical and experimental drags for TH04

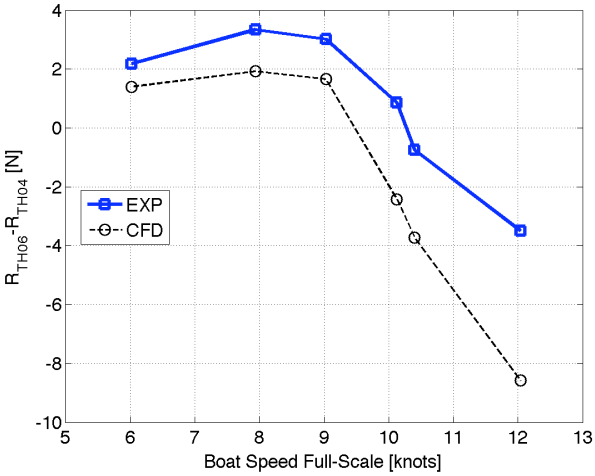

Figure 4: Drag differences between the TH06 and TH04 models.

Conclusions

In the present paper the hydrodynamic performance of two America's Cup hulls were computed with CFD and compared with towing tank data. The uncommon characteristics of this comparison are that it was performed: with fully appended hulls; in *free to sink and trim* conditions; not knowing *a priori* the experimental data for one of the two hulls.

The numerical/experimental differences of the drag are of the order of 1%, whilst sink and trim variations are computed with an accuracy of the order of 1 mm and 0.01 deg respectively. If the experiment or the computations were used to choose the boat with the lower resistance, the same choice would have been made for most of the boat speeds. In a small boat speed range, around 10 knots full scale, the experiment and the CFD would have led to different choices. The differences between the numerical results and the measured data are of the same order of magnitude as the accuracy of the experimental results. Hence the choice between the two hulls at 10 knots would be debatable.

Several simulations of the first hull were performed, comparing numerical results with experimental data, which were known *a posteriori*. This allowed the effect of several computational parameters to be investigated and their effect to be discussed.

Grids: hexahedral non-structured non-conformal grids and block structured conformal grids were tested. The two grid types perform similarly and not one of them could be recommended above the other. Grids with a number of cells from 700,000 to 2,000,000, with $y+$=30, allow the accuracy required in yacht design practice to be achieve.

Discretization Order: use of first order is suggested for the transient terms, whilst second order is suggested for the convection terms. Using second order in time led to instabilities, whilst using first order in space led to drag over-estimation.

6DOF: the pitching inertia and the distance from the bow to the upstream boundary face can be used to decrease the oscillation of the solution.

Skin Friction: it is recommended that the proposed alternative method to compute the skin friction, which takes into account the *numerical ventilation,* is used.

Time Steps from ts=0.02s to ts=0.0001s were tested. Decreasing the time step causes the *numerical ventilation* to decrease, which leads the friction drag to increase. However, if the friction drag is computed with the proposed method, which takes into account the *numerical ventilation*, the friction drag decreases due to lower numerical diffusion.

Acknowledgments

The support of CD-adapco is gratefully acknowledged. In particular, the authors are grateful to Demetris Clerides and Anthony Massobrio for supporting the project, to Carlo Pettinelli for his suggestions, and to Paul Bosauder (Matrix Applied Computing Ltd) for a high-quality technical support.

References

[1] Azcueta R, Computational of Turbulent Free Surface Flows Around Ships and Floating Bodies, PhD Thesis, Technical University Hamburg-Harburg, Germany, 2001.

[2] Brown M, Campbell I, Robinson J, The Accuracy and Repeatability of Tank Testing, from Experience of ACC Yacht Development, in the proceedings of The 1st High Performance Yacht Design Conference, Auckland, New Zealand, 4th-6th December 2002.

[3] Imas L, Baker B, Ward B, Buley G, CFD-Based Hydrodynamic Analysis of High Performance Racing Yachts, In the proceedings of The 19th Chesapeake Sailing Yacht Symposium, Annapolis, Maryland, pp. 31-36, 20th-21st March 2009.